SEE COMMENTARY

Targeted evolution of pinning landscapes for large superconducting critical currents

Ivan A. Sadovskyy[a], Alexei E. Koshelev[a], Wai-Kwong Kwok[a], Ulrich Welp[a], and Andreas Glatz[a,b,1]

[a]Materials Science Division, Argonne National Laboratory, Argonne, IL 60439; and [b]Department of Physics, Northern Illinois University, DeKalb, IL 60115

Edited by Laura H. Greene, Florida State University, Tallahassee, FL, and approved March 12, 2019 (received for review October 10, 2018)

The ability of type II superconductors to carry large amounts of current at high magnetic fields is a key requirement for future design innovations in high-field magnets for accelerators and compact fusion reactors, and largely depends on the vortex pinning landscape comprised of material defects. The complex interaction of vortices with defects that can be grown chemically, e.g., self-assembled nanoparticles and nanorods, or introduced by postsynthesis particle irradiation precludes a priori prediction of the critical current and can result in highly nontrivial effects on the critical current. Here, we borrow concepts from biological evolution to create a vortex pinning genome based on a genetic algorithm, naturally evolving the pinning landscape to accommodate vortex pinning and determine the best possible configuration of inclusions for two different scenarios: a natural evolution process initiating from a pristine system and one starting with preexisting defects to demonstrate the potential for a postprocessing approach to enhance critical currents. Furthermore, the presented approach is even more general and can be adapted to address various other targeted material optimization problems.

genetic algorithms | targeted selection | superconductivity | vortex pinning | critical current

Life has undergone tremendous changes due to natural selection—from relatively simple molecules with replication capability to complex organisms, whose understanding is still far beyond present contemplation. Modern computer systems have enabled the effective exploitation of the idea of natural selection for practical purposes. The underlying genetic algorithms are widely used in electromagnetic and mechanical design, financial mathematics, energy applications, scheduling problems, circuit design, image processing, medicine, etc. Within this approach, one only needs to specify the direction of positive mutations to find optimal or beneficial characteristics of the system of interest, i.e., replace natural evolution by targeted evolution, which is especially effective in complex systems with a large number of degrees of freedom.

A key science aspect to advance the deployment of high-temperature superconductors (HTSs) is the discovery of novel materials that can carry large currents without dissipation at high-magnetic fields (1). These materials are especially desirable for high-performance applications (2) such as superconducting motors, generators, magnets, and power lines in urban areas (3–5). Low dissipation is also very important for superconducting cavities for particle accelerators (6), undulators for x-ray synchrotrons (7), and compact fusion reactors (8). The main challenge is to suppress the dissipation in these systems caused by the motion of quantized elastic magnetic flux tubes or vortices, which appear in type II superconductors in magnetic fields above the first critical field (9). Since most applied superconductors are of type II, the study of efficient pinning mechanisms benefits a majority of superconducting technologies. Vortices can be pinned (or trapped) by inhomogeneities in the material, usually in the form of nonsuperconducting defects (10). Examples are point-like pinning centers (impurities, vacancies, inclusions), 1D defects (dislocations, irradiation tracks), or 2D defects (twin boundaries, stacking faults). Although extensive knowledge has been gained in the pursuit of high critical currents (the highest current the system can carry without dissipation) (11–15), the fundamental solution to the dynamics of interacting vortices in disordered media is still unknown. Only recently more systematic, computer-assisted approaches were developed (16, 17), leading to the critical-current-by-design methodology (18).

While sophisticated numerical optimization methods (19) and corresponding experiments can guide the design of superconductors with enhanced critical current densities (J_c), the problem requires defining the general geometry of the vortex pinning landscape (or pinscape) a priori. This works well if only a certain type of pinning defects is present—in other words, pinscapes defined by only a few parameters. Hence, the overall best pinscape for the highest J_c cannot be determined by these approaches. To address this question, one needs to study all possible combinations of defects, resulting in highly mixed pinscapes. Each of the individual defects are described by numerous material and geometrical parameters, resulting in an extremely high-dimensional parameter space for the pinscape. This is where evolutionary concepts can be used.

In this work, we borrow concepts from biological evolution to create a vortex pinning genome with targeted evolution for predicting high in-field J_c. We focus on the geometrical aspect of the defects to produce the best pinscape for a given system. In particular, we evolve the pinscape by changing the shapes of individual defects (see sketch of targeted evolution in Fig. 1), thereby

Significance

Lossless transport is the Holy Grail of energy science in general and superconductivity research in particular. The main obstacle is the dissipative motion of Abrikosov vortices, which can be reduced or eliminated by pinning at nonsuperconducting defects. Pinning effectiveness nontrivially depends on various factors such as the shape, concentration, and spatial distribution of defects, rendering the optimization of the vortex pinning landscape highly difficult. Here, we use concepts from biological evolution to develop an efficient strategy for vortex pinning improvement. We replace natural selection with targeted selection, where only pinning configurations with better vortex immobilization survive. In combination with high-performance numerical algorithms, it allows us to dynamically evolve the defect landscape into the best possible pinning configuration with maximal lossless current.

Author contributions: I.A.S., W.-K.K., U.W., and A.G. designed research; I.A.S., A.E.K., and A.G. performed research; I.A.S. and A.G. contributed new reagents/analytic tools; I.A.S. and A.G. analyzed data; and I.A.S., A.E.K., W.-K.K., U.W., and A.G. wrote the paper.

The authors declare no conflict of interest.

This article is a PNAS Direct Submission.

This open access article is distributed under Creative Commons Attribution-NonCommercial-NoDerivatives License 4.0 (CC BY-NC-ND).

See Commentary on page 10201.

[1]To whom correspondence should be addressed. Email: glatz@anl.gov.

This article contains supporting information online at www.pnas.org/lookup/suppl/doi:10.1073/pnas.1817417116/-/DCSupplemental.

Published online April 8, 2019.

Downloaded at Palestinian Territory, occupied on December 7, 2021

www.manaraa.com

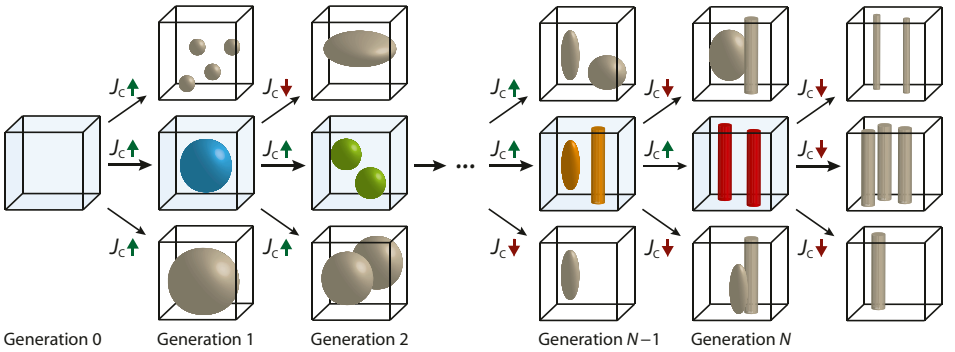

Fig. 1. Sketch of a targeted evolution of the pinning landscape. We start with generation 0, which contains a single configuration without defects. Each defect has elliptical shape and is characterized by three independent diameters. The evolution process mutates the pinning landscape by adding/removing, translating, scaling, and reshaping particles. These mutations create the next generation. We accept the pinning landscape with maximal critical current density (J_c) and discard all others. The evolution ends at some generation N with configuration having maximal J_c (shown in red).

including the possibility of all major defect types such as columnar and spherical defects, which can be experimentally realized. Moreover, our approach can also be adapted for many different materials optimization/design problems. Here, we demonstrate its power for (*i*) numerically determining the maximum possible J_c in superconductors with nonmagnetic normal inclusions and (*ii*) developing a universal postprocessing strategy for enhancing the performance of superconductors with preexisting pinning landscapes such as in commercial HTS wires and superconductors in alternating or nonhomogeneous magnetic fields.

Targeted Evolution

An essential ingredient for our approach is to obtain the critical current for a given evolved pinscape. Here, we describe the collective dynamics and pinning of vortices by the time-dependent Ginzburg–Landau equation (TDGLE), allowing us to determine J_c (16, 17)—the fitness function. The TDGLE yields J_c as function of shapes, sizes, and positions of pinning defects (see details in *SI Appendix*).

As a quite general model, we consider pinning landscapes containing D ellipsoidal metallic pinning centers with principle axes (a_i, b_i, c_i), aligned in the x, y, and z directions, with center positions (x_i, y_i, z_i), where $i = 1, \ldots, D$. These ellipsoidal defects can describe a large variety of defect geometries in superconductors such as precipitates, point defects, dislocations, grain boundaries, and stacking faults, as well as particle irradiation-induced columnar or spherical defects. For example, point defects can be modeled by small spherical inclusions, grain boundaries by flattened spheroids and columnar defects by spheroids with one of the diameters larger than the system size. To find pinscapes with ellipsoidal defects that yield the highest J_c, we use an evolution-based algorithm with three distinct stages: mutations and targeted selection (stage 1), extrapolation and analysis (stage 2), and verification (stage 3), described below.

Stage 1: Mutations and Targeted Selection. This step implements the evolutionary paradigm, during which the shape and position of individual inclusions is altered independently (mutation) and J_c is calculated. A set of random mutations produces a new generation. Each new pinscape or successor may contain one (typical) or more sequential mutations (rare). Each pinscape is evaluated, and the one with the largest J_c is chosen for further evolution (see sketch in Fig. 1). The initial pinscape usually depends on the problem to be studied. For a general situation (discussed in the next section), one can initiate the targeted evolution algorithm with an empty pinscape, the 0th generation, which represents an infinite homogeneous system with zero J_c.

Mutations have random type, strength, direction, and number of affected inclusions, namely: (*i*) copying of existing inclusions or adding new inclusions of random shape; (*ii*) removing inclusions; (*iii*) changing the inclusion principle axes a_i, b_i, and c_i; (*iv*) changing the inclusion position (x_i, y_i, z_i); (*v*) repelling/attracting pairs of inclusions, i.e., increasing/decreasing the distance between randomly chosen inclusions i and j; (*vi*) squishing inclusions, i.e., changing the inclusion's axes a_i, b_i, and c_i while maintaining its volume; (*vii*) splitting inclusions, i.e., creating a pair of inclusions with the same volume as the original one; and (*viii*) merging pairs of inclusions. Mutation types (*vi*) to (*viii*) preserve the volume of the affected inclusions. Note, that if we start the mutation process with an empty pinscape, the only possible mutation is the addition of defects. We calculate J_c for each pinscape in a generation. These are then compared with the maximal J_c of the previous generation. In case none of the mutations increase J_c, we repeat the mutation procedure and expand the population in the current generation until at least one pinscape produces a J_c larger than the maximal critical current of the previous generation or a maximum population is reached. This stage is implemented to work in parallel. If a configuration with larger J_c is found within a generation, we select the pinscape with the largest J_c as the seed configuration for the following generation and then apply the mutation procedure again. Repeating this protocol produces subsequent generations of pinscapes with even higher J_c. We stop in generation N if no further J_c enhancement is found (the cutoff population size is 2,048).

The evolution approach provides us with the types and parameters of defects that ensure maximum vortex pinning and, consequently, maximum J_c. The results are obtained without any assumptions of the pinscape structure and only depend on external parameters such as magnetic field and temperature. In some application relevant situations, the initial pinscape and the type of possible mutations may have some constraints, which we address below.

Stage 2: Extrapolation and Analysis. Stage 1 provides information regarding the distribution of the particle sizes and, in some cases, their spatial distribution. We can model/extrapolate these distributions with only a few parameters such as the size and typical distances between defects. In other words, one can use the general knowledge of the defect shapes obtained by the evolutionary approach and characterize the corresponding pinscape with a simplified global parameter set. For example, if the optimal pinscape consists of randomly distributed spherical defects of similar diameters, the configuration can be characterized by two parameters: concentration and diameter of the defects (16).

Downloaded at Palestinian Territory, occupied on December 7, 2021
www.manaraa.com

Based on the simplified global parameter set, near-optimal pinscapes can be fine-tuned using conventional optimization methods (19). Furthermore, one can sample J_c for near-optimal parameter sets to determine the robustness of the configuration and compare them to analytical results (10, 20).

Stage 3: Verification. To test the model obtained in stage 2, we restart the evolution process with the best model configuration and change the positions and sizes of each inclusion individually. The model is verified, if subsequent evolution cannot further increase J_c by a significant amount (we typically use a threshold of 3% within 2,048 mutations).

Stages 2 and 3 are in a sense optional, as they elucidate the underlying mechanism for the optimal pinscape, extract a model, and show the stability of the process. Stage 1 alone can determine the general optimal pinscapes.

Pinning Landscape for Maximal Critical Current Density in Fixed Field. Starting with empty pinscapes and allowing almost any possible mutation is usually not very relevant for applications. However, it is instructive to study this case as it ultimately yields the best pinning configurations for given external parameters. Consider the exemplary situation of a fixed magnetic field applied along the z axis (or c axis in HTSs) and current flowing along the x direction. Naïvely, the optimal pinning landscape should mimic the vortex configuration for zero applied current at the given field, namely the Abrikosov vortex lattice. Hence, the pinscape should be a hexagonal array of columnar defects, with each column trapping a single vortex. However, the evolutionary approach yields an even better pinscape: a periodic array of planar pinning defects (walls) that are aligned with the current and field direction (here parallel to the xz plane).

In the simulation, we apply a constant external magnetic field $B = 0.1H_{c2}$ at low temperatures, corresponding to nearly zero noise (reduced temperature $T_f = 10^{-5}$; see ref. 21 for details). Inclusions are modeled by a nonsuperconducting material with zero critical temperature, $T_{c,i}$, resulting in a suppressed order parameter, $\psi(\mathbf{r})$, inside the defects. Here, H_{c2} is the upper critical field at given temperature.

Following the evolution approach described above, an actual evolution process for of an initially empty pinscape is illustrated in Fig. 2. Note that J_c rises faster in early generations; improvements in later generations require more mutations and lead to a smaller gain in J_c. The evolution terminates with the 37th generation and results in a set of almost equidistant planar defects oriented in the direction of applied current and having a thickness on the order of a coherence length (Fig. 2*B*). The distance between planar defects roughly corresponds to positions of vortex rows in a perfect hexagonal lattice (blue circles) generated by the external magnetic field. The full evolution tree has 37 generations and 6,331 pinning configurations (Fig. 2*C*). The best landscapes in each generation are numbered and have color ranges from blue with almost zero J_c to orange with maximal $J_c = 0.40J_{dp}$, where J_{dp} is the depairing current. Each

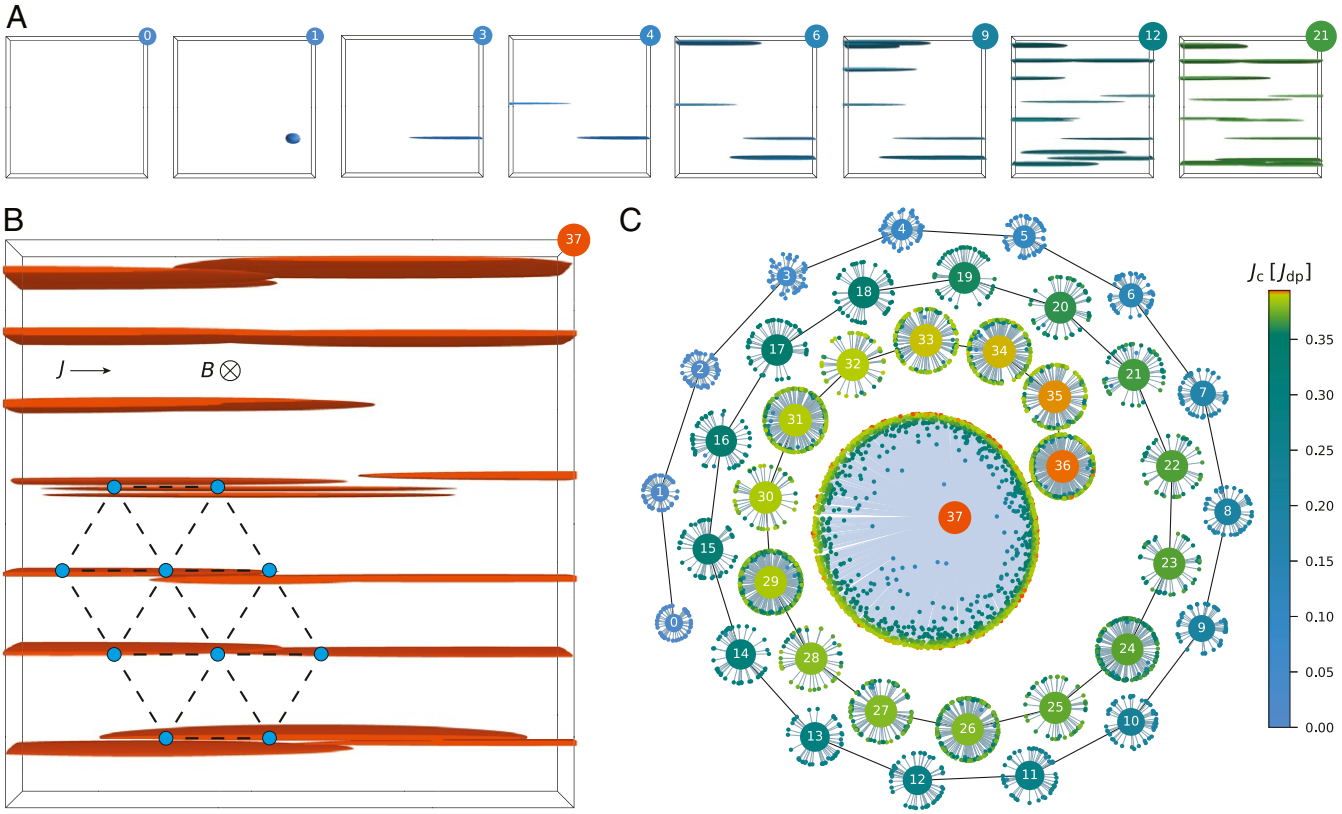

Fig. 2. Evolution history. (*A*) The evolution process starts with a superconductor without inclusions shown in the left panel. The following panels show pinning landscapes having highest J_c in first, third, fourth, sixth, ninth, 12th, and 21st generation, correspondingly. In the first generation, the maximal J_c is achieved with the configuration containing a single nearly spherical inclusion. In second and third generations, this inclusion evolves to a flattened ellipsoid lying in the plane spanned by the current and magnetic field. In subsequent generations, this ellipsoid is copied multiple times to enhance the total pinning. The remaining generations of the evolution process fine tunes the landscape by copying, removing, moving, and slightly deforming successors of the seed inclusion. (*B*) The final pinning landscape consisting of a periodic array of almost planar defects has the best possible J_c in the framework of our model. The positions of pinned vortices are shown schematically by blue circles. (*C*) The evolution tree. The numbered circles represent configurations with the maximum J_c per generation. Dead mutations are indicated by dots. All J_c values are color-coded.

SEE COMMENTARY
PHYSICS
Downloaded at Palestinian Territory, occupied on December 7, 2021
www.manaraa.com

numbered configuration has at least 20 successors: (*i*) the successor with maximum J_c becomes the numbered seed for the next generation; (*ii*) all other successors are shown by small colored circles. These configurations have smaller J_c values than the seed and are discarded by our targeted selection. The final 37th configuration in the center has 2,040 mutations with smaller J_c values. The vast majority (90%) of these dead mutations lead to marginal decreases of J_c (from 1 to 15%, shown in green). Therefore, the determined configuration, shown in Fig. 2*B*, is rather stable with respect to mutation.

The used parameters produce a rather large critical current, $J_c(T) = 0.40 J_{dp}(T)$, at almost zero temperature. For a larger noise level ($T_f = 0.28$) corresponding to a temperature $T \sim 77$ K, $J_c(T)$ reduces to $0.34 J_{dp}(T)$. Weaker metallic pinning centers with higher critical temperature, e.g., $T_{c,i} = 2T - T_{c,b}$ ($T_{c,b}$ is the critical temperature in the bulk superconductor) can produce a maximal $J_c = 0.31 J_{dp}$ at zero noise. In all these cases, we can easily extrapolate a model for the optimal pinning configuration with only two parameters: the thickness of the planar defects and their separation.

Based on the optimal pinscape, we studied the critical dynamics close to J_c (see *SI Appendix*, Fig. S1 and Movies S1–S3 for corresponding order parameter and supercurrent densities). Namely, the depinning process involves the collective motion of vortices, which effectively increases the pinning force of the system. The same collective behavior occurs for other types of J_c-optimized pinning landscapes, e.g., for ordered defects (22) or disordered nanorods extended along the direction of the applied magnetic field (18). A similar but somewhat less pronounced effect was observed for randomly placed spherical particles (16). We conclude that the collective depinning in very-large-J_c systems leads to a much more pronounced and sharp transition to the dissipative state than individual vortex depinning in suboptimal pinscapes, confirmed by current–voltage curves (*SI Appendix*, Fig. S2 and Movies S3 and S4).

Our targeted evolution derived pinning landscape with $J_c = 0.40 J_{dp}$ can be compared with other typical pinscapes with potentially high J_c at the same magnetic field $B = 0.1 H_{c2}$ and low thermal noise: (*i*) randomly placed spherical defects with optimal diameter and concentration have a maximum possible J_c of $0.061 J_{dp}$ (16); (*ii*) field-aligned, randomly placed columnar inclusions with the best diameter and concentration lead to $J_c = 0.091 J_{dp}$ (19); (*iii*) hexagonally ordered, field-aligned columnar defects with optimal size and concentration generate a significantly larger critical current $J_c = 0.32 J_{dp}$ but still smaller than for planar defects.

Next, we compare the properties of hexagonally ordered columnar with that of arrays of planar defects—the idealized model derived from the genetic approach.

Planar vs. Columnar Defects. A systematic comparison of a hexagonal lattice of columnar defects to the extrapolated model of a periodic array of planar defects requires comparable parameters. The natural parameters for columnar defects are the matching field B_Φ (the hypothetic magnetic field producing an Abrikosov vortex lattice with the same density as the lattice of columns) and their diameter d. For arrays of planar defects, one can use the same matching field B_Φ and place the defects along one of the

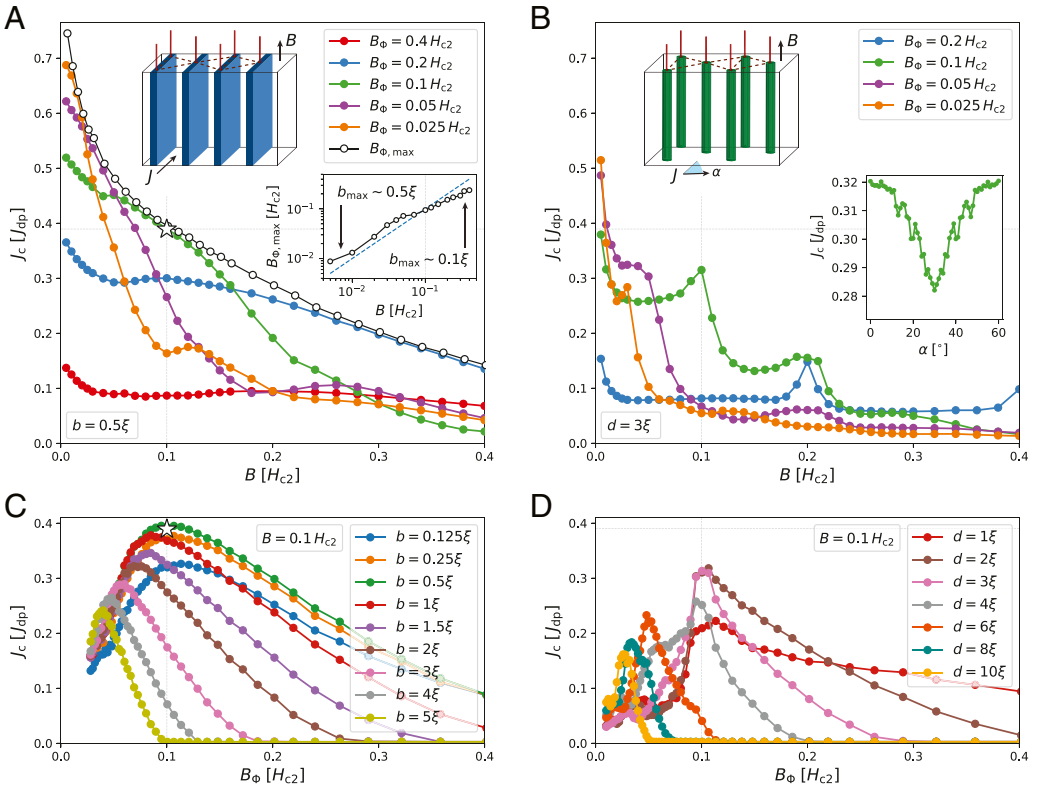

Fig. 3. Critical current as a function of magnetic field, $J_c(B)$, for different landscapes and matching fields B_Φ. (*A*) Planar defects with fixed thickness of $b = 0.5\xi$ and range of B_Φ from 0.025 to $0.4 H_{c2}$. The star shows the targeted evolution result for $B = 0.1 H_{c2}$. The envelope curve (black line with open circles) shows the maximal possible $J_{c,max}(B)$ at a given field B. *Inset* shows the corresponding optimal matching field $B_{\Phi,max}$, i.e., the distance needed to achieve this maximum. (*B*) Hexagonal pattern of columnar defects with diameter $d = 3\xi$. *Inset* shows J_c as a function of hexagonal lattice rotation angle α with respect to the applied current. It is $\pi/3$-periodic and maximal if the current is aligned with the lattice axes. (*C*) J_c as a function of matching field for planar defects in applied field $B = 0.1 H_{c2}$ for different wall thicknesses, b. (*D*) The same for columnar defects ordered in a hexagonal pattern for different diameters, d, of the columns.

Downloaded at Palestinian Territory, occupied on December 7, 2021
www.manaraa.com

SEE COMMENTARY

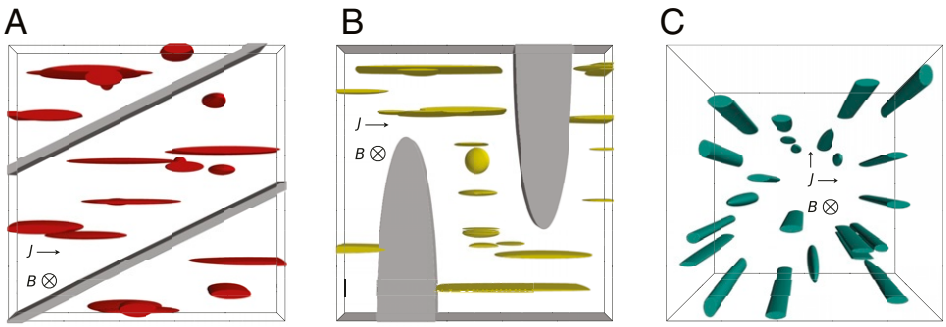

Fig. 4. Pinscape evolution for predefined environments. (*A*) Current is applied from left to right, and magnetic field is fixed at $B = 0.1H_{c2}$ perpendicular to the figure plane as in Fig. 2. The difference is in the preexisting pinscapes containing tilted planar defects shown in gray. These plates redirect the supercurrent flow (boundary conditions are periodic in the figure plane) and make the optimal pinscape shown in Fig. 2 inefficient. The evolutionary approach generates smaller planar defects (or flat cylinders) along the current between the preexisting inclusions. (*B*) In this scenario, two flattened half-cylinders block the current with open (no-current) boundary conditions at the top and bottom surfaces. Generated inclusions are more cylindrical between inclusions to avoid blocking supercurrents. (*C*) In this scenario, the current can be applied in left–right and bottom–up directions, and the largest critical current is defined by the minimum critical current in either direction. The pinscape evolves to hyperuniformly placed columnar defects.

main axes (parallel to the current) of the hexagonal lattice (and along the field) (Fig. 3 *A* and *B*, *Insets*). The distance between the planar defects is then $h = 3^{1/4}\xi(\pi H_{c2}/B_\Phi)^{1/2}$, i.e., $3^{1/2}/2$ less than for columnar defects. The second parameter is the thickness of the planar defects. In both cases, the maximum J_c is reached when $B = B_\Phi$ (Fig. 3 *C* and *D*). A main difference is that the planar array is more robust against changes in B_Φ than the discrete columnar defects structure, i.e., small changes in B_Φ (or h) result in very small changes in the optimal J_c.

Fig. 3*A* shows the $J_c(B)$ dependence for the planar array with fixed thickness, $b = 0.5\xi$, and different B_Φ ranging from $0.025H_{c2}$ to $0.4H_{c2}$. All curves display a relatively smooth behavior. The most representative is the green curve simulated for $B_\Phi = 0.1H_{c2}$; the open star on the green curve corresponds to J_c associated with the pinning landscape shown in Fig. 2*B* obtained by targeted evolution for $B = 0.1H_{c2}$. For the green curve $J_c(B') \geqslant J_c(0.1H_{c2})$ for all $B' \leqslant 0.1H_{c2}$; this property persists for all reasonable wall-pattern parameters with optimized B_Φ and b at a given field B, i.e. $J_c(B') \geqslant J_c(B)$ for $B' \leqslant B$. The envelope curve (black line with circles) shows $J_{c,\max}(B)$, the critical current for optimized landscapes for each fixed B with optimal wall thickness $b(B)$ and matching field $B_{\Phi,\max}(B)$. The deviation of $B_{\Phi,\max}(B)$ from a simple linear dependence $B_\Phi = B$ (*Inset*) is due to different $b(B)$, ranging from $\sim 0.5\xi$ at low fields to $\sim 0.1\xi$ at higher fields.

Fig. 3*B* shows the $J_c(B)$ dependence for hexagonal-patterned columnar defects with fixed diameter $d = 3\xi$ for different B_Φ from $0.025H_{c2}$ to $0.2H_{c2}$. The green curve shows a peak at the first matching field with $J_c = 0.32J_{dp}$, which coincides with the maximal J_c of the hexagonal lattice at $B = 0.1H_{c2}$. A rotation of the hexagonal pattern can reduce this value (it is maximum if a main axis of the lattice is aligned with the current; see angular dependence in *Inset*).

Fig. 3*C* depicts the $J_c(B_\Phi)$ dependence for arrays of planar defects with different wall thickness b at fixed applied field $B = 0.1H_{c2}$. This sampling shows a single robust optimum near $B_\Phi = 0.1H_{c2}$ and $b = 0.5\xi$. A similar sampling for the hexagonal columnar defect pattern presented in Fig. 3*D* shows significantly sharper peaks in the vicinity of the matching field, resulting in less robust behavior against small changes of the parameters. Samplings for other parameters are shown in *SI Appendix*, Figs. S4–S8.

Application-Relevant Examples of Targeted Evolution

A recent report on doubling J_c of commercial HTS wire by additional particle irradiation (23) highlights the importance and advantages of a postsynthesis approach to enhance J_c, while leaving the wire synthesis process untouched. Our targeted evolution approach can also be applied to systems with preexisting defects. Fig. 4 demonstrates results of targeted evolution in different environments, defined by either preexisting pinscapes or different external parameters. In Fig. 4 *A* and *B*, we apply the evolutionary algorithm to pinscape with fixed preexisting defects. These defects partially block the left-to-right current flow and, thus, dramatically change the result of the targeted evolution described above. Mainly, the evolution leaves some defect-free regions in the superconducting matrix to allow for a supercurrent path. In the case of preexisting tilted walls in Fig. 4*A*, the total current $I_c = J_c wt$ through the system was increased by evolution from $I_c = 56J_{dp}\xi^2$ ($J_c = 0.11J_{dp}$) to $I_c = 147J_{dp}\xi^2$ ($J_c = 0.29J_{dp}$) in applied field $B = 0.1H_{c2}$, where $w = 64\xi$ and $t = 8\xi$ are the system's width and thickness, respectively. In the case of the preexisting two half-ellipses shown in Fig. 4*B*, the critical current rises, from $I_c = 35J_{dp}\xi^2$ ($J_c = 0.068J_{dp}$) to $I_c = 104J_{dp}\xi^2$ ($J_c = 0.20J_{dp}$) upon evolution of added defects.

In Fig. 4*C*, we apply the current both in the horizontal and vertical directions and consider the fitness function $J_{c,u} = \min\{J_{c\rightarrow}, J_{c\uparrow}\}$, where $J_{c\rightarrow}$ is left-to-right J_c and $J_{c\uparrow}$ is bottom-to-up J_c, rather than only $J_{c\rightarrow}$ as before. $J_{c,u}$ approximately models arbitrary directions of applied currents. The resulting pinscape consists of columnar defects along the magnetic field arranged in a hyperuniform pattern (22, 24). The corresponding critical current density, $J_c = 0.27J_{dp}$, is 5% less than the J_c for a hexagonal lattice oriented in the wrong way (rotated $\pi/6$ from the main axes; see the angular dependence in Fig. 3*B*, *Inset*).

In all of the simulations above, we intentionally did not limit the size, shape, or placement of the mutated defects. However, it is possible to limit the defect morphology to mimic the limitations of practical postprocessing procedures.

Discussion and Conclusions

In this paper, we introduced an evolutionary approach for the optimization of pinscapes in type II superconductors. This approach utilizes the idea of targeted selection inspired by biological natural selection. We demonstrated that it can be applied to enhance the current-carrying capacity of superconductors in a magnetic field.

We discovered that certain patterns of defects composed of metallic inclusions can maximize the critical current up to 40% of J_{dp} for fixed direction of the current perpendicular to the magnetic field at 10% of H_{c2}. We numerically demonstrated

PHYSICS
Downloaded at Palestinian Territory, occupied on December 7, 2021
www.manaraa.com

that no other mixture of different defect shapes can reach this level of J_c. The discussed pining structure may arise in niobium titanium wires, in which a sequence of heating/drawing steps result in a microstructure composed of nanometer-scale metallic and almost parallel α-titanium lamellae embedded in the niobium titanium matrix (25). Furthermore, the layered structure of cuprate HTSs give rise to intrinsic pinning of similar nature.

In contrast to conventional optimization techniques such as coordinate descent, where one varies only a few parameters characterizing the entire sample (e.g., size and concentration of defects), our targeted evolution approach allows us to vary each defect individually without any a priori assumptions about the defects configuration. This flexibility outweighs its higher computational cost. The considered optimization problem has basically infinite degrees of freedom, prompting one to ask why the evolution method convergences relatively quickly. One reason is that there are a lot of configurations with J_c quite close to the maximum possible one, which are in practice, indistinguishable from each other. The evolutionary approach just allows us to find one such configuration. Typically, larger regions of near-optimum configurations correspond to a broader maximum of J_c as a function of a set of appropriate parameters, e.g., the system in Fig. 3*C* evolutionally adapts faster than the system in Fig. 3*D*.

We also demonstrated the enhancement of J_c for two cases of preexisting defects, found in commercial HTSs. Our approach provides a computer-assisted route to rational enhancement of the critical current in applied superconductors. It can be used to define a postsynthesis optimization step for existing state-of-the-art HTS wires for high-field magnet applications by modeling the actual geometry of the wire within the magnet and taking into account external magnetic field distributions and self-fields. This can be done by coupling transport simulations with Maxwell equations and initiating the simulation with a preexisting defect distribution in the wire.

Finally, we note that the described evolutionary algorithm is a local method and thus can easily get stuck in a local maximum. An analog in biological evolution is the extreme detour of a giraffe's recurrent laryngeal nerves (26), which became trapped under the aortic arch in the thorax. However, in contrast to natural selection, targeted evolution can be performed multiple times. Namely, a comparison of the resultant pinscapes and corresponding J_c values allows us to estimate how close they are to the best possible pinscape, making targeted evolution global. Moreover, by finding different near-maximum points, it is possible to understand which parameters are important for large J_c and which ones are not. An experimental analog in organic systems is the process of in vitro selection (27). A particular example is the selection of RNA molecules being able to bind to specific ligands (28): it was shown that evolved molecules bind stronger than those of the first generation and an a priori guess of the best binding RNA sequence would not have been possible.

In conclusion, our methodology of using targeted evolutionary concepts to improve the intrinsic properties of condensed matter systems is a promising path toward the design of tailored functional materials. It can be applied to a large variety of different physical systems and has demonstrated its usefulness in the enhancement of superconducting critical currents. Furthermore, its ability to take existing environments into account allows for optimization by postprocessing.

Materials and Methods

The evolutionary algorithm was implemented in Python, and the TDGLE simulations were implemented for high-performance computers with general-purpose graphics processing unit coprocessors; see details and used parameters in *SI Appendix*.

ACKNOWLEDGMENTS. We thank L. Civale, R. Willa, and I. S. Aranson for numerous useful comments. I.A.S., A.E.K., and A.G. were supported by the Scientific Discovery through Advanced Computing program, funded by US Department of Energy (DOE), Office of Science, Advanced Scientific Computing Research and Basic Energy Science, Division of Materials Science and Engineering. U.W. and W.-K.K. were supported by the Center for Emergent Superconductivity, an Energy Frontier Research Center funded by the US DOE, Office of Basic Energy Sciences. Simulations were performed at the Oak Ridge Leadership Computing Facility (LCF) (DOE Contract DE-AC05-00OR22725), the Argonne LCF (DOE Contract DE-AC02-06CH11357), and the Computing Facility at Northern Illinois University.

1. Campbell AM, Evetts JE (1972) Flux vortices and transport currents in type II superconductors. *Adv Phys* 21:199–428.
2. Kwok WK, et al. (2016) Vortices in high-performance high-temperature superconductors. *Rep Prog Phys* 79:116501.
3. Malozemoff AP (2012) Second-generation high-temperature superconductor wires for the electric power grid. *Annu Rev Mater Res* 42:373–397.
4. Senatore C, et al. (2014) Progresses and challenges in the development of high-field solenoidal magnets based on RE123 coated conductors. *Supercond Sci Technol* 27:103001.
5. Obradors X, Puig T (2014) Coated conductors for power applications: Materials challenges. *Supercond Sci Tech* 27:044003.
6. Padamsee HS (2014) Superconducting radio-frequency cavities. *Annu Rev Nucl Part Sci* 64:175–196.
7. Kesgin I, Kasa M, Ivanyushenkov Y, Welp U (2017) High-temperature superconducting undulator magnets. *Supercond Sci Technol* 30:04LT01.
8. Kramer D (2015) New MIT design revives interest in high-field approach to fusion. *Phys Today* 68:23–24.
9. Abrikosov A (1957) On the magnetic properties of superconductors of the second group. *Sov Phys JETP* 5:1174–1182.
10. Blatter G, Feigel'man MV, Geshkenbein VB, Larkin AI, Vinokur VM (1994) Vortices in high-temperature superconductors. *Rev Mod Phys* 66:1125–1388.
11. Dew-Hughes D (1974) Flux pinning mechanisms in type II superconductors. *Philos Mag* 30:293–305.
12. Kes P (1992) *Flux pinning and the summation of pinning forces. Concise Encyclopedia of Magnetic & Superconducting Materials*, ed Evetts J (Pergamon Press, Oxford), pp 163–171.
13. Scanlan RM, Malozemoff AP, Larbalestier DC (2004) Superconducting materials for large scale applications. *Proc IEEE* 92:1639–1654.
14. Godeke A, ten Haken B, ten Kate HHJ, Larbalestier DC (2006) A general scaling relation for the critical current density in Nb_3Sn. *Supercond Sci Technol* 19: R100–R116.
15. Foltyn S, et al. (2007) Materials science challenges for high-temperature superconducting wire. *Nat Mat* 6:631–642.
16. Koshelev AE, Sadovskyy IA, Phillips CL, Glatz A (2016) Optimization of vortex pinning by nanoparticles using simulations of the time-dependent Ginzburg-Landau model. *Phys Rev B* 93:060508.
17. Sadovskyy IA, et al. (2016) Simulation of the vortex dynamics in a real pinning landscape of $YBa_2Cu_3O_{7-\delta}$ coated conductors. *Phys Rev Appl* 5:014011.
18. Sadovskyy IA, et al. (2016) Toward superconducting critical current by design. *Adv Mater* 28:4593–4600.
19. Kimmel G, Sadovskyy IA, Glatz A (2017) In silico optimization of critical currents in superconductors. *Phys Rev E* 96:013318.
20. Willa R, Geshkenbein VB, Blatter G (2016) Probing the pinning landscape in type-II superconductors via Campbell penetration depth. *Phys Rev B* 93:064515.
21. Sadovskyy IA, Koshelev AE, Phillips CL, Karpeyev DA, Glatz A (2015) Stable large-scale solver for Ginzburg-Landau equations for superconductors. *J Comp Phys* 294:639–654.
22. Sadovskyy IA, Wang YL, Xiao ZL, Kwok WK, Glatz A (2017) Effect of hexagonal patterned arrays and defect geometry on the critical current of superconducting films. *Phys Rev B* 95:075303.
23. Jia Y, et al. (2013) Doubling the critical current density of high temperature superconducting coated conductors through proton irradiation. *Appl Phys Lett* 103:122601.
24. Le Thien Q, McDermott D, Reichhardt CJO, Reichhardt C (2017) Enhanced pinning for vortices in hyperuniform pinning arrays and emergent hyperuniform vortex configurations with quenched disorder. *Phys Rev B* 96:094516.
25. Lee PJ, Larbalestier D (2003) Niobium-titanium superconducting wires: Nanostructures by extrusion and wire drawing. *Wire J Int* 36:61–66.
26. Barnosky AD (2010) Giraffe–nervous system. *Mammal Anatomy: An Illustrated Guide* (Marshall Cavendish, New York), pp 74–75.
27. Jijakli K, et al. (2016) The in vitro selection world. *Methods* 106:3–13.
28. Ellington AD, Szostak JW (1990) In vitro selection of RNA molecules that bind specific ligands. *Nature* 346:818–822.

Downloaded at Palestinian Territory, occupied on December 7, 2021
www.manaraa.com